Proc. Natl. Acad. Sci. USA
Vol. 84, pp. 7802–7806, November 1987
Biochemistry

Chromatin higher-order structure studied by neutron scattering and scanning transmission electron microscopy

S. E. GERCHMAN AND V. RAMAKRISHNAN

Biology Department, Brookhaven National Laboratory, Upton, NY 11973

Communicated by Gary Felsenfeld, May 27, 1987 (received for review January 15, 1987)

ABSTRACT **Neutron scattering in solution and scanning transmission electron microscopy were simultaneously done on chicken erythrocyte chromatin at various salt and magnesium concentrations. We show that chromatin is organized into a higher-order structure even at low ionic strength and that the mass per unit length increases continuously as a function of salt concentration, reaching a limiting value of between six and seven nucleosomes per 11 nm. There is no evidence of a transition from a 10-nm to a 30-nm fiber. Fiber diameter is correlated with mass per unit length, showing that both increase during condensation. We also find that there is no essential difference between the mass per unit length measured by scanning transmission electron microscopy and neutron scattering in solution, showing that the ordered regions seen in micrographs are representative of chromatin in solution.**

Nucleosomes in chromatin interact to form a higher-order structure, referred to as the 30-nm filament. Despite a large number of structural studies on chromatin, there is no unanimity on its higher-order structure. The nature and sources of conflicting views of the structure of the 30-nm fiber have been summarized (1).

Several models of the 30-nm fiber propose a helical structure for chromatin. These include the solenoidal model (2), the helical-ribbon model (3, 4), the crossed-linker double-helical model (5), and the nonsequential single-helix model (6). All of these models share certain similarities; for example, they all satisfy constraints imposed by electric dichroism measurements on the angle of the nucleosomal disk with respect to the fiber axis (7, 8). Most of the models have similar repeat dimensions that would show up as peaks in a diffraction pattern. The helical-ribbon model predicts certain additional peaks due to the width of the ribbon. These additional peaks have not been observed in an experiment on oriented chromatin (9), but it is possible that an adjustment in the parameters of the helical-ribbon model would eliminate the additional reflections that are predicted.

Despite such similarities, the models differ considerably in detail. Even at a coarse level, the various models predict different values for the mass per unit length of condensed chromatin. Thus a measurement of the physical characteristics of chromatin condensation could help to substantiate or rule out some of the existing models for chromatin structure.

The mass per unit length of chromatin has been measured by small-angle scattering (10–14). The parameter has also been measured by hydrodynamic methods (7, 15) and light scattering (16). These experiments generally yield a value of 6–7 nucleosomes per 11 nm for the mass per unit length of the condensed 30-nm fiber. However, scanning transmission electron microscopy (STEM) studies on chromatin (4, 5) have yielded much higher values, of up to 11.6 nucleosomes per nm. Felsenfeld and McGhee (1) have pointed out that the discrepancy may be due to the fact that in STEM studies one selects ordered regions of chromatin, whereas physical studies on chromatin in solution yield parameters that are the average for chromatin as a whole.

The condensation of chromatin as a function of monovalent and divalent cation concentration has also been studied extensively. In their original model, Finch and Klug (2) proposed that at low ionic strength, chromatin exists as a loose filament of ≈100 Å in diameter. This form of chromatin has been referred to as the 10-nm filament. It was proposed that as ionic strength is increased, chromatin undergoes a transition from the 10-nm filament to the 30-nm fiber found under physiological ionic conditions. A neutron-scattering study (13) reports evidence for this transition, by measuring a very different cross-sectional radius of gyration at low and high ionic strength. Other studies on chromatin have observed a transition as a function of ionic strength (17–20).

In this study, we have sought to answer the following questions regarding chromatin structure. What is the mass per unit length of chromatin, and how does the measured mass per unit length depend on whether the technique is selective (as in STEM) or averaging (as in neutron scattering)? What is the nature of condensation of chromatin with ionic strength?

We have used small-angle neutron scattering to measure the mass per unit length and cross-sectional radius of gyration to chromatin fibers. We have concurrently made STEM measurements of mass per unit length on the same samples. The result is that differences due to sample preparation and source of chromatin have been completely eliminated.

MATERIALS AND METHODS

Preparation of Soluble Chicken Erythrocyte Chromatin. Chicken erythrocyte nuclei were isolated from fresh, heparinized blood by the method of Hewish and Burgoyne (21). All steps were carried out at 0–4°C, and all buffers contained 0.1 mM phenylmethylsulfonyl fluoride and 0.1 mM benzamidine added immediately before use. The nuclei were adjusted to a concentration of 125 A_{260} units/ml in a buffer containing 60 mM KCl, 15 mM NaCl, 0.15 mM spermine, 0.5 mM spermidine, 15 mM 2-mercaptoethanol, 0.34 M sucrose, and 15 mM Tris·HCl (pH 7.4). They were then digested for 30 min at 4°C with micrococcal nuclease at 240 units/ml in the presence of 1 mM $CaCl_2$. The digestion was stopped by the addition of 1/100 vol of 0.2 M EDTA.

Soluble chromatin was isolated by lysing the nuclei in 25–30 mM NaCl/10 mM Tris·HCl/0.2 mM EDTA, pH 7.5. The yield of soluble chromatin was roughly 25% of the total. The chromatin was arbitrarily separated into three size classes (low, medium, and high molecular weight) on 10–29% (wt/wt) isokinetic sucrose gradients containing 25 mM NaCl, 10 mM Tris·HCl (pH 7.5), and 0.2 mM EDTA. Each gradient was loaded with 300 A_{260} units of chromatin and centrifuged at 28,000 rpm, 4°C, for 2.5 hr in a Beckman SW28 rotor. Only

The publication costs of this article were defrayed in part by page charge payment. This article must therefore be hereby marked "*advertisement*" in accordance with 18 U.S.C. §1734 solely to indicate this fact.

Abbreviations: STEM, scanning transmission electron microscopy; TMV, tobacco mosaic virus.

the high molecular weight chromatin was used for subsequent study. The chromatin was concentrated, when necessary, using vacuum filtration through a dialysis membrane with a M_r 60,000 cut-off (Biomolecular Dynamics). Recoveries from concentration varied between 70 and 90%. Methods such as ultrafiltration through a stirred pressure cell resulted in the chromatin being deposited as a gel on the membrane.

The size distribution of the DNA from the resulting chromatin was determined by electrophoresis on 0.5% agarose gels and then measuring the fluorescence after staining with ethidium bromide. A *Cla* I digest of T7 DNA was used to calibrate the migration distance in terms of molecular weight. The distribution peaked around 22 kilobases; over 75% of the DNA was longer than 17 kilobases. The percent of chromatin that remains soluble in a given buffer was measured by dialysis into various salt concentrations (overnight), followed by low-speed centrifugation (10,000 × *g*, 10 min) to remove any precipitated chromatin. The chromatin used in this study was insoluble when the NaCl concentration exceeded 125 mM, or when the magnesium concentration (in the presence of 40 mM NaCl) exceeded 1 mM, at pH 7.5.

Neutron Scattering. Neutron scattering was done on the H9B spectrometer of the High Flux Beam Reactor at Brookhaven National Laboratory (22). Samples were dialyzed into the appropriate buffers at a DNA concentration of 2–5 mg/ml. Cylindrical quartz cells of 1-mm thickness were used to contain the samples for scattering. Data collected on a two-dimensional position-sensitive detector were corrected for background and buffer scattering, normalized for beam intensity, for transmission, and for concentration, and radially integrated. This yielded the scattered intensity $I(q)$ as a function of $q = 4\pi \sin \theta/\lambda$, where λ is the wavelength and 2θ is the scattering angle. Cross-sectional Guinier plots ($\ln[qI(q)]$ vs. q^2) were analyzed to yield the forward scatter $[qI(q)]_0$ and the cross-sectional radius of gyration R_x. Incoherent scattering from water was used to calibrate the scattered intensity on an absolute scale (23). This allowed a determination of mass per unit length from the forward scatter.

Electron Microscopy. The same samples that were used for neutron-scattering experiments were used for STEM mass measurements, except that for STEM the concentration was much lower (≈0.2–2 A_{260} units). The samples were fixed in 0.5% glutaraldehyde in the appropriate buffer at 0°C. The time of fixation varied between 1 and 16 hr. In some cases the glutaraldehyde was dialyzed out before layering on the grid. Neither this dialysis nor the time of fixation within the range specified affected the mass measurements significantly, although dialyzing out the glutaraldehyde after an hour of fixation resulted in a slightly lower background.

Preparation of samples for measurements at the STEM facility of Brookhaven National Laboratory was done as described by Wall and Hainfeld (24). The samples were underlayed on thin carbon films by the wet-film technique and freeze-dried. The dose varied between 10 and 15 electrons per Å^2. The apparent mass was measured using tobacco mosaic virus (TMV) for mass calibration. Apparently straight and ordered regions of chromatin fibers were chosen for mass analysis, and a histogram of mass per unit length measurements was used to calculate a mean for the sample.

RESULTS

Electron Microscopy. Fig. 1 shows examples of STEM micrographs of chromatin under various conditions. The pictures obtained are similar to those obtained by Woodcock *et al.* (4). Chromatin depleted of H1 and H5 (stripped chromatin) by the method of Kaplan *et al.* (25) appears to be randomly coiled with many long uncoiled stretches (Fig. 1*A*).

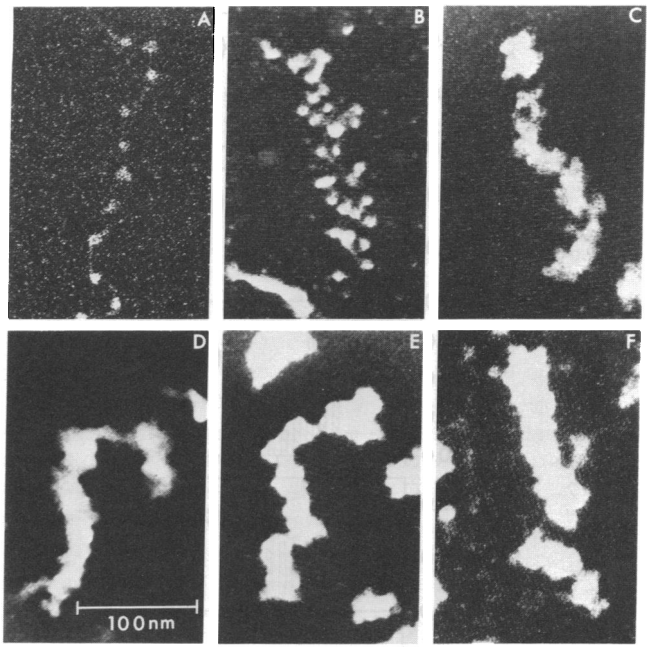

FIG. 1. Examples of scanning transmission electron micrographs of chromatin in various NaCl and $MgCl_2$ concentrations. All buffers contained 5 mM Hepes, pH 7.5. Several buffers (*A–E*) also contained 0.2 mM EDTA. (*A*) Stripped chromatin in 0 mM NaCl. (*B–F*) Native chromatin in 0 mM NaCl, 60 mM NaCl, 80 mM NaCl, 120 mM NaCl, and 0.8 mM $MgCl_2$/40 mM NaCl.

Stripped chromatin does not show any organization even at higher ionic strengths (data not shown). Native chromatin on the other hand shows a loose but definite organization of nucleosomes into a higher-order structure even at low ionic strength (Fig. 1*B*). There is also a compaction of chromatin with ionic strength (Fig. 1*C–E*) and with magnesium (Fig. 1*F*).

STEM mass measurements have generally relied on tobacco mosaic virus (TMV) as a calibration standard (25). For chromatin at low ionic strength, individual nucleosomes are visible in the field making it possible to measure the apparent mass per nucleosome. The measured mass per nucleosome for native chromatin is 324 kDa per nucleosome, which is ≈25% larger than the calculated value of 258 kDa per nucleosome for chicken erythrocyte chromatin. Evidently, calibration with TMV grossly overestimates the measured mass per nucleosome in the presence of H1 and H5. However, for stripped chromatin the measured mass per nucleosome of 250 kDa per nucleosome is close to the calculated value of 238 kDa per nucleosome. For our mass per unit length measurements on chromatin fibers, we have used the ratio of the measured to the calculated mass per nucleosome as a normalization factor, to correct the apparent mass obtained by using TMV as a standard. The results, therefore, yield a value for nucleosomes per nanometer that is independent of the calibration standard.

Fig. 2 shows histograms of the mass per unit length measurements for chromatin in various concentrations of NaCl and magnesium ions.

Neutron Scattering. The cross-sectional radius of gyration R_x and the mass per unit length M_1 of long rods can be measured directly by small-angle scattering (26). Neutron small-angle scattering has a special advantage over x-ray scattering: the low coherent scattering density of H_2O for neutrons means that neutron-scattering measurements in H_2O are quite insensitive to hydration effects and changes in the partial specific volume (e.g., see ref. 23). This means that the mass per unit length and diameter of chromatin fibers can

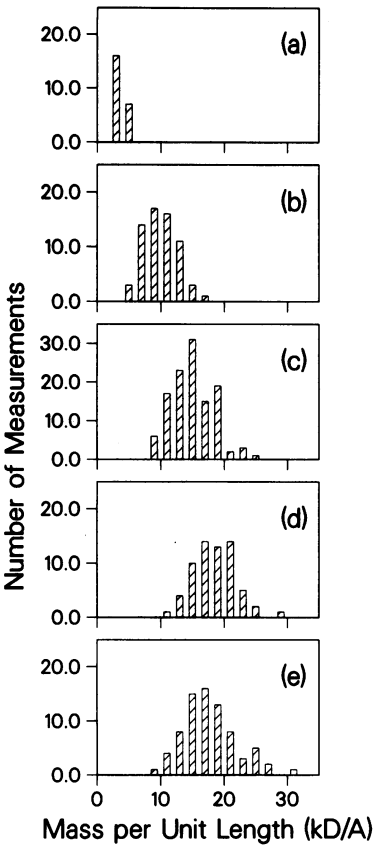

FIG. 2. Histograms of STEM measurements of the mass per unit length of chromatin fibers in various concentrations of salt and magnesium. (*a*) 0 mM NaCl. (*b*) 60 mM NaCl. (*c*) 80 mM NaCl. (*d*) 120 mM NaCl. (*e*) 0.8 mM $MgCl_2$/40 mM NaCl. A, Å.

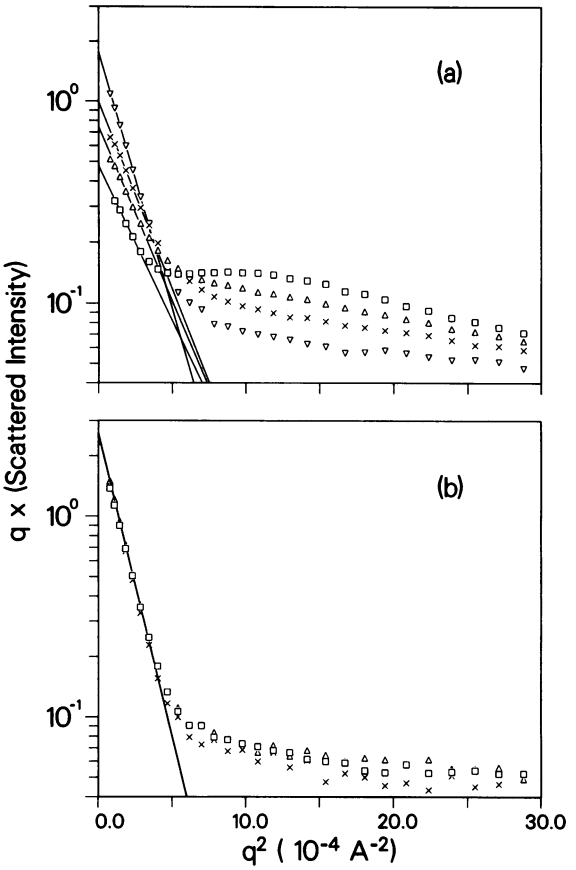

FIG. 3. Small-angle neutron-scattering data on chromatin. The ordinate shows on a logarithmic scale the product of the scattering vector q and the scattered intensity. The scattered intensity is measured in units of neutrons scattered per unit solid angle, normalized for beam intensity, sample thickness, transmission, and concentration. The abscissa shows the square of the scattering vector. The straight line in each case shows a weighted least-squares fit to the low-angle part of the curve. The intercept of this line on the y-axis is proportional to the mass per unit length, and the slope is proportional to the square of the cross-sectional radius of gyration. All buffers contained 5 mM Hepes and 0.2 mM EDTA, pH 7.5 as well as NaCl as follows. (*a*) □, 10 mM NaCl; △, 20 mM NaCl; ×, 30 mM NaCl; ▽, 60 mM NaCl. (*b*) □, 80 mM NaCl; △, 100 mM NaCl; ×, 120 mM NaCl. A, Å.

be measured over a wide range of ionic strengths without having to worry about associated changes in hydration or partial specific volume.

Examples of cross-sectional Guinier plots of chromatin are shown in Fig. 3. The low-angle part of the data were fit to a straight line, and the mass per unit length M_1 and cross-sectional radius of gyration R_x were calculated from the intercept and slope, respectively. The data show that as the salt concentration is increased, there is a change in the scattering curve for chromatin with a concomitant increase in the mass per unit length and the cross-sectional radius of gyration (Fig. 3*a*). However, for NaCl concentrations greater than 80 mM, a limiting structure is reached (Fig. 3*b*); the scattering curves for 80 mM, 100 mM, and 120 mM NaCl are nearly identical. Chromatin in increasing magnesium concentrations reaches a similar limiting structure.

Variation of Mass per Unit Length with Ionic Strength. Fig. 4*a* shows the variation of the mass per unit length of chromatin with NaCl concentration, as measured by small-angle scattering and STEM, whereas Fig. 4*b* shows similar data as a function of magnesium ion concentration. In both cases, the neutron scattering data show that the mass per unit length reaches a limiting value of between six and seven nucleosomes per 11 nm. The STEM measurements in Fig. 4*a* do not by themselves provide evidence of a limiting value of mass per unit length. The measurements are too few and with too much scatter to detect saturation. However, it is clear that the STEM measurements are scattered about the curve representing neutron-scattering data, showing that the two methods are in good agreement. The STEM measurement yields a somewhat higher value at 120 mM NaCl, but, given the scatter of the STEM values about the neutron-scattering curve, it is doubtful that the difference is significant. The single STEM value in Fig. 4*b* is also slightly higher than the comparable neutron-scattering value but, nevertheless, is in reasonable agreement.

Variation of Fiber Diameter with Mass per Unit Length. Fig. 5 shows the variation of the mass per unit length with the cross-sectional radius of gyration. These data were obtained by using the values for M_1 and R_x from all the small-angle scattering experiments done on chromatin in different NaCl and Mg^{2+} concentrations. The data show a definite correlation between R_x and M_1. The relationship appears to be roughly linear. Since the fiber diameter is proportional to the cross-sectional radius of gyration, the data indicate that the fiber diameter is roughly proportional to the mass per unit length.

DISCUSSION

The mass per unit length and the cross-sectional radius of gyration of chromatin vary continuously with ionic strength (Figs. 3 and 4). Even at the lowest ionic strength, the measured radius of gyration of 70 Å is too large to be compatible with the expected 25–30 Å for a 10-nm filament. This is evidence that chromatin is organized into a higher-

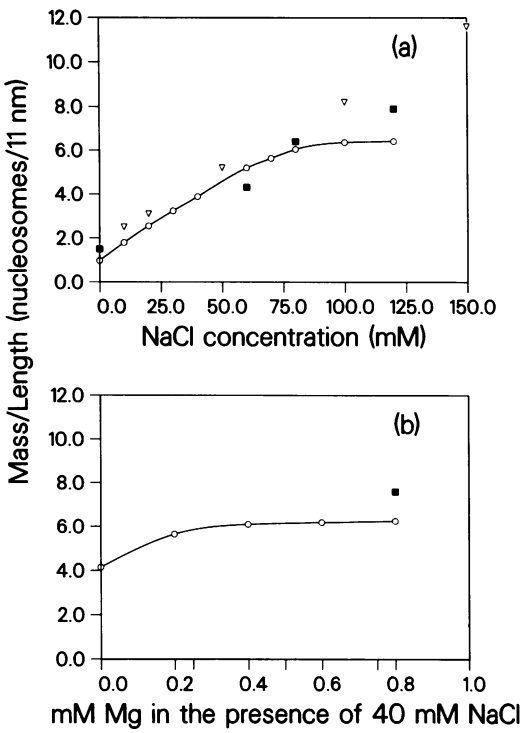

FIG. 4. Variation of mass per unit length with NaCl and $MgCl_2$ concentration. ○, Mass per unit length obtained from neutron-scattering measurements in solution; ■, STEM measurements on the same sample; ▽, values obtained by Woodcock *et al.* (4) by STEM.

order structure even at low ionic strength. Our data do not support a 10-nm to 30-nm transition as a function of salt concentration. Our data fully support x-ray scattering measurements (14, 27) but are in conflict with some reports (13, 20) in which the published data at low ionic strength do not extend to sufficiently low angles and in which it is possible that the inner slope was missed. In such cases, a slope measured at higher angles measures correlations over shorter distances such as 10 nm. It is thus characteristic of local regions of the fiber and not of chromatin as a whole. A detailed critique of the earlier experiments can be found in a review (28). The general applicability of Guinier analysis to fibers of finite length and nonuniform cross section has been examined by Hjelm (29). His work has established the validity of the use of this technique for chromatin.

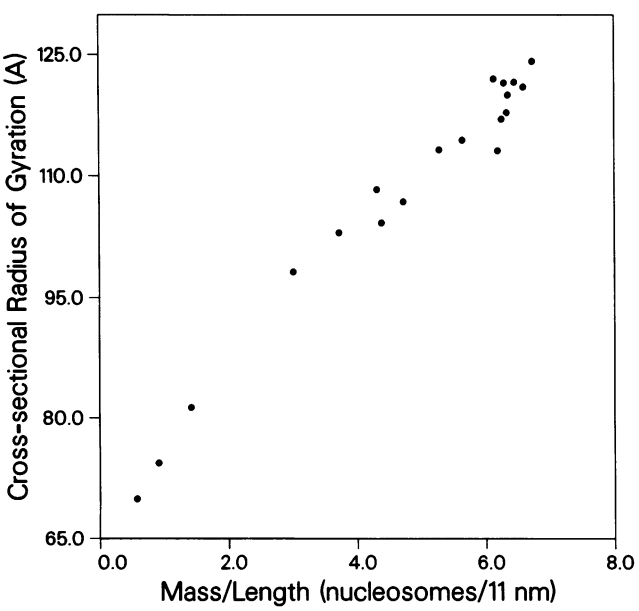

FIG. 5. Correlation of the cross-sectional radius of gyration (which is proportional to the fiber diameter) with the mass per unit length of chromatin. The correlation implies that the fiber diameter must increase as chromatin condenses from its more extended form at low ionic strength to its compact form in higher salt concentrations. The points represent data from various neutron-scattering measurements in a variety of salt and magnesium concentrations. A, Å.

A transition as a function of ionic strength has been observed in the sedimentation experiments of Thomas and her coworkers (17–19). However, there is no conflict between our data and theirs. The sedimentation data indicate that the transition does not occur for chromatin fragments <50 nucleosomes long but is observed for longer chromatin. The authors propose that the transition is seen not because of a sudden change in the higher-order structure but is due to the greater susceptibility of longer fragments to hydrodynamic shear. If these fragments are stabilized at high ionic strength, one would see a transition as a function of salt concentration. Our data fully support this explanation, since the chromatin in our scattering measurements is not being subjected to shear, and in any case, the cross-sectional radius of gyration and the mass per unit length measured by small-angle scattering would not be influenced significantly by breaks in the fiber.

The measured mass per unit length in solution appears to saturate between six and seven nucleosomes per 11 nm, in agreement with many physical studies of chromatin in solution (e.g., see refs. 7, 13, 15, and 16). In Fig. 4 the curve representing scattering measurements levels off, showing that the chromatin has reached a state of maximal compaction. Thus we would not expect to measure a significantly higher mass per unit length by going to higher NaCl or Mg^{2+} concentration.

Fig. 4 shows that while there is more scatter in the STEM measurements, in general, the mass per unit length determined by STEM and neutron scattering on the same samples agree quite well. The greater smoothness of neutron data is not surprising, since such data yield average parameters for the entire population of chromatin molecules in the beam. Fig. 4*a* also shows STEM data of Woodcock *et al.* (4) on the mass per unit length of chromatin. Whereas our values are systematically lower than those of Woodcock *et al.* (4) the disagreement is small until a salt concentration of 100 mM NaCl is reached. Our values start to level off by 100 mM NaCl, whereas those of Woodcock *et al.* (4) continue to increase roughly linearly with salt concentration. The major disagreement occurs at 150 mM NaCl, where Woodcock *et al.* (4) obtain a mass per unit length that is almost twice the value we get at 120 mM NaCl. We were unable to make a measurement at 150 mM NaCl because most of our chromatin precipitates in this salt concentration, but it is apparent from our neutron scattering data that the mass per unit length of our chromatin has reached its maximal value before that. In our study, there is no significant difference in parameters obtained from solution scattering and STEM. This indicates that the ordered regions chosen for STEM analysis are representative of the state of chromatin in solution. It also indicates that discrepancies that exist between earlier STEM and solution studies are not because STEM selects ideal "ordered" structures, whereas physical measurements in solution average over both ordered and disordered regions.

The reasons for the discrepancy between earlier STEM measurements and the data presented here remain nebulous, and we merely enumerate the possibilities. The main area of disagreement with Woodcock *et al.* (4) occurs in a range where our chromatin is mostly insoluble. It is possible that earlier STEM measurements were influenced by aggregation

of chromatin fibers. However, Williams *et al.* (5) made their measurements in 70 mM NaCl, where most chromatin is soluble. Calibration with TMV could lead to an overestimate of the mass per unit length of chromatin fixed with glutaraldehyde, although, this by itself is not enough to explain the discrepancy of almost a factor of two. Morever, Williams *et al.* (5) took the same calibration precautions that we did. There is a good deal of heterogeneity in the mass per unit length of chicken erythrocyte chromatin (see Fig. 2), resulting in some subjectivity in STEM regarding the choice of "ordered" regions. It is possible that different workers use slightly different criteria for analysis, leading to a small but systematic difference in the parameters obtained. While the source of chromatin could be a possible reason for differences between the work of Williams *et al.* (5) and ourselves, this would not apply to the work of Woodcock *et al.* (4) who also used chicken erythrocyte chromatin. It is unlikely that any of the possibilities mentioned above could by itself explain the discrepancy with earlier STEM studies. They might combine, however, to systematically affected STEM mass measurements in the same direction. Finally, it could be argued that the chromatin in our study has not reached its full state of compaction and, therefore, results in a lower mass per unit length compared to the previous STEM studies. In view of the fact that our neutron-scattering data show that a limiting structure is reached, we consider this unlikely.

The correlation of cross-sectional radius of gyration, R_x, with mass per unit length (Fig. 5) shows that the fiber diameter must increase as chromatin condenses into its most compact state. In the crossed-linker model of Langmore and his coworkers (5), condensation of chromatin could not occur merely by an increase in the twist of the ribbon formed by a double array of nucleosomes. Such a condensation mechanism predicts that the fiber diameter remains fairly constant as the mass per unit length increases, which our data do not support. Within the context of the model, condensation must occur by a change in both the angle of the linker DNA with respect to the fiber axis (thus changing the diameter of the fiber as a whole) as well as an increase in the twist of the ribbon of nucleosomes. Also, our data do not support the high mass per unit length that is possible in this model, but it is of course possible that constraints other than merely steric ones operate to limit the amount of twist in the nucleosomal array.

Attempts have been made to fit small-angle scattering data to detailed models. Because several models could fit such data reasonably well, the uniqueness of models cannot be proved using these measurements. A similar caution applies to interpreting various features of solution-scattering data, such as bumps at characteristic spacings. For example, the same feature has been interpreted as arising from the pitch of a helix (27) or as characteristic of the diameter of the fiber (5). In our opinion, such approaches are unlikely to prove fruitful.

The experiments reported here place general constraints on any model of chromatin higher-order structure. The data are compatible with the solenoidal model for chromatin. They are also compatible with other models such as the one proposed by Staynov (6) that differs from the solenoidal model primarily in the connectivity of adjacent nucleosomes and predicts a more modest mass per unit length than the limiting values of the helical-ribbon or the crossed-linker models (4, 5).

This work was supported by the Office of Health and Environmental Research of the U.S. Department of Energy. Suport for the Brookhaven STEM is provided by Grant RR 01777 from the National Institutes of Health and the U.S. Department of Energy. We thank Kristin Elmore and Grace Shiue for preparing specimens for STEM measurements. We thank Paul Furcinitti, Frank Kito, Jim Hainfeld, and Joe Wall for help with STEM measurements and analysis and for useful suggestions. We are grateful to Dieter Schneider for critical comments and help with neutron experiments.

1. Felsenfeld, G. & McGhee, J. D. (1986) *Cell* **44,** 375–377.
2. Finch, J. T. & Klug, A. (1976) *Proc. Natl. Acad. Sci. USA* **73,** 1897–1901.
3. Worcel, A., Strogatz, S. & Riley, D. (1981) *Proc. Natl. Acad. Sci. USA* **78,** 1461–1465.
4. Woodcock, C. L. F., Frado, Y. L. L. & Rattner, J. B. (1984) *J. Cell Biol.* **99,** 52–52.
5. Williams, S. P., Athey, B. D., Muglia, L. J., Schappe, R. S., Gough, A. H. & Langmore, J. P. (1986) *Biophys. J.* **49,** 233–248.
6. Staynov, D. Z. (1983) *Int. J. Biol. Macromol.* **5,** 3–10.
7. McGhee, J. D., Nickol, J. M., Felsenfeld, G. & Rau, D. C. (1983) *Cell* **33,** 831–841.
8. Mitra, S., Sen, D. & Crothers, D. M. (1984) *Nature (London)* **308,** 247–249.
9. Widom, J. & Klug, A. (1985) *Cell* **43,** 207–213.
10. Sperling, L. & Tardieu, A. (1976) *FEBS Lett.* **64,** 89–91.
11. Baudy, P. & Bram, S. (1978) *Nucleic Acids Res.* **5,** 3698–3713.
12. Hollandt, H., Hotbohm, H., Riedel, F. & Harbers, E. (1979) *Nucleic Acids Res.* **6,** 2017–2027.
13. Suau, P., Bradbury, E. M. & Baldwin, J. P. (1979) *Eur. J. Biochem.* **97,** 593–602.
14. Bordas, J., Perez-Grau, L., Koch, M. H. J., Vega, M. C. & Nave, C. (1986) *Eur. Biophys. J.* **13,** 157–173.
15. Butler, P. J. G. (1984) *EMBO J.* **3,** 2599–2604.
16. Campbell, A. M., Cotter, R. I. & Pardon, J. F. (1978) *Nucleic Acids Res.* **5,** 1571–1580.
17. Thomas, J. O. (1984) *J. Cell. Sci.*, Suppl. 1, 1–20.
18. Butler, P. J. G. & Thomas, J. O. (1980) *J. Mol. Biol.* **140,** 505–529.
19. Bates, D. L., Butler, P. J. G., Pearson, E. C. & Thomas, J. O. (1981) *Eur. J. Biochem.* **119,** 469–476.
20. Greulich, K. O., Wachtel, E., Ausio, J., Seger, D. & Eisenberg, H. (1986) *J. Mol. Biol.*, in press.
21. Hewish, D. R. & Burgoyne, L. A. (1973) *Biochem. Biophys. Res. Commun.* **52,** 504–510.
22. Schneider, D. & Schoenborn, B. P. (1984) in *Neutrons in Biology*, ed. Schoenborn, B. P. (Plenum, New York), pp. 119–142.
23. Jacrot, B. & Zaccai, G. (1981) *Biopolymers* **20,** 2413–2426.
24. Wall, J. S. & Hainfeld, J. F. (1986) *Annu. Rev. Biophys. Chem.* **15,** 355–376.
25. Kaplan, L. J., Gauer, R., Morrison, E., Langan, T. A. & Fasman, G. D. (1984) *J. Biol. Chem.* **259,** 8777–8785.
26. Porod, G. (1982) in *Small Angle X-Ray Scattering*, eds. Glatter, O. & Kratky, O. (Academic, New York), pp. 17–53.
27. Perez-Grau, L., Bordas, J. & Koch, M. H. J. (1984) *Nucleic Acids Res.* **12,** 2987–2995.
28. Koch, M. H. J. & Sayers, Z. (1986) in *Biophysics and Synchrotron Radiation*, ed. A. Bianconi (Springer, Berlin), in press.
29. Hjelm, R. P. (1985) *J. Appl. Crystallogr.* **18,** 452–460.